Collins-Soper kernel from lattice QCD at the physical pion mass

arXiv:2307.12359

Artur Avkhadiev[1]

in collaboration with

Phiala Shanahan[1], Michael Wagman[2], and Yong Zhao[3]

1 Massachusetts Institute of Technology

2 Fermilab

3 Argonne National Laboratory

Meeting on Lattice Parton Physics from Large Momentum Effective Theory

University of Regensburg,

July 24–26, 2023

TMD Physics and the Collins-Soper kernel

- Transverse motion of partons in hadrons gives rise to TMD functions, encoded in hadronic lightcone matrix elements.
- The Collins-Soper (CS) kernel governs RG evolution of any TMD along the scale ζ:

$$\phi_{p/h}(x, b_T, \mu, \zeta) = \phi_{p/h}(x, b_T, \mu, \zeta_0) \exp\left[\frac{1}{2}\gamma_p(b_T, \mu) \ln \frac{\zeta}{\zeta_0}\right]$$

Fourier conjugate to parton's transverse momentum.

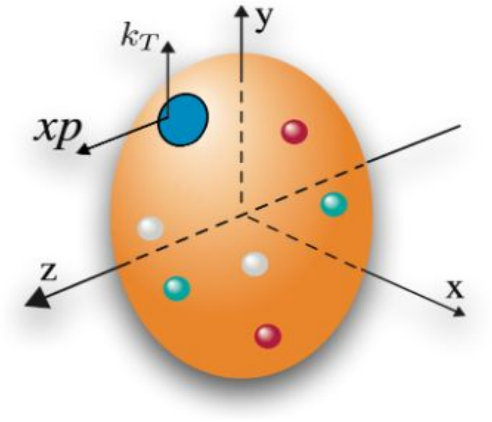

Fig. from TMD Handbook (modified).

- The scale ζ is related to the hadron's momentum p

$$\gamma_p(b_T, \mu) = \frac{2}{\ln(\zeta_1/\zeta_2)} \frac{\phi_{p/h}(x, b_T, \mu, \zeta_1)}{\phi_{p/h}(x, b_T, \mu, \zeta_2)}$$

- ~ Ratio of lightcone matrix elements at different ζ ~ p
- Non-perturbative

Goal: LQCD + LaMET for direct comparison with global analyses

- Consistent for $b_T \lesssim 0.2\,\mathrm{fm}\,(\approx 1\,\mathrm{GeV}^{-1})$
- Non-perturbative modeling significant for $b_T \gtrsim 0.2\,\mathrm{fm}$, to be improved with EIC data.
- **LQCD + LaMET goal:** sufficient precision for comparison or input to future global analyses.

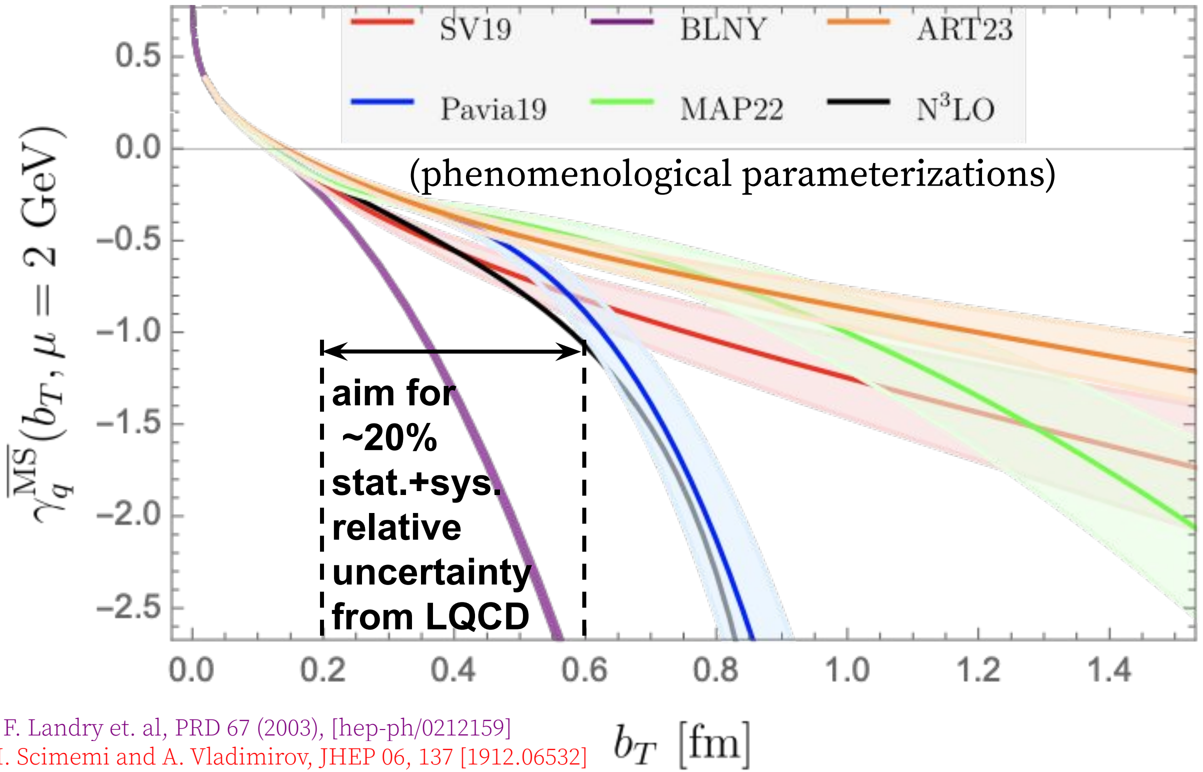

BLNY: F. Landry et. al, PRD 67 (2003), [hep-ph/0212159]
SV19: I. Scimemi and A. Vladimirov, JHEP 06, 137 [1912.06532]
Pavia19: A. Bacchetta et. al, JHEP 07, 117, [1912.07550]
MAP22: A. Bacchetta et. al, JHEP 10, 127, [2206.07598]
ART23: V. Moos et. al, [2305.07473]

Status of our group's LQCD calculations of the CS kernel

LQCD calculations evolving from proof of concept toward improved systematic uncertainties

- $M_\pi \approx 540\,\mathrm{MeV},\ 0.12\,\mathrm{fm} \le b_T \le 0.48\,\mathrm{fm}$
- Dominated by Fourier Transform systematics
- **NLO** matching

- $M_\pi \approx 150\,\mathrm{MeV},\ 0.12\,\mathrm{fm} \le b_T \le 0.86\,\mathrm{fm}$
- Improved Fourier Transform systematics
- **NNLL** matching

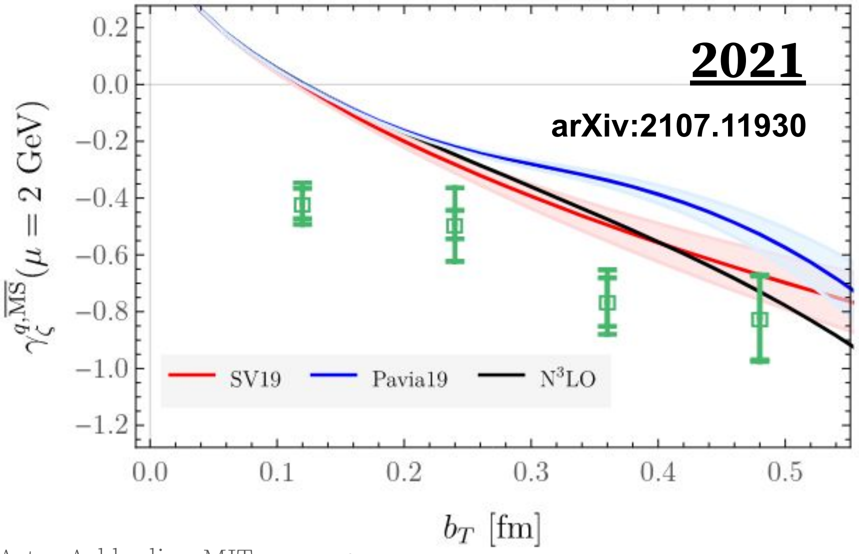

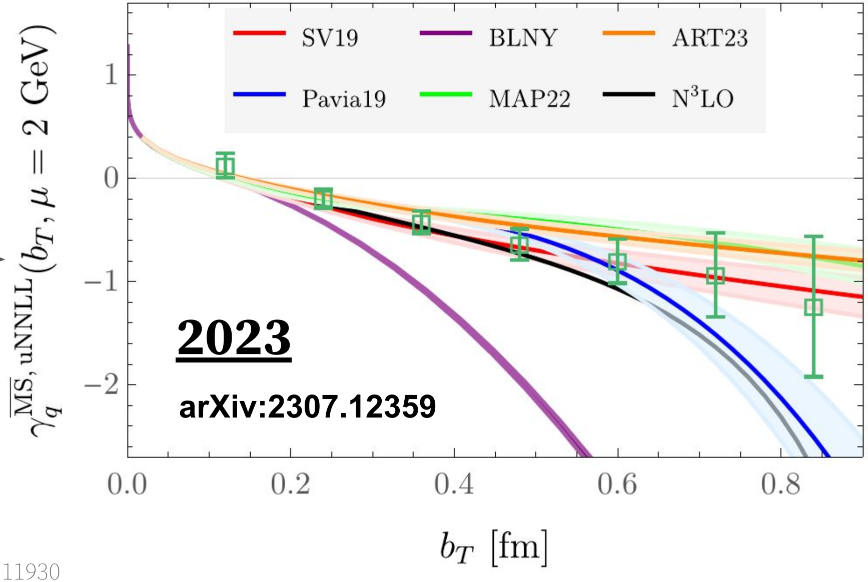

Fig. from Shanahan, Wagman, Zhao, Phys.Rev.D 104 (2021), 2107.11930

Improvements in CS kernel estimate from LQCD

X. Ji et. al., Phys. Lett. B 811 [1911.03840]

Continuum limit (to be done)

Fourier Transform with improved systematics

Position-space quasi-TMD WFs at close-to-physical pion mass

$$\gamma_q(\mu, b_\mathrm{T}) = \boxed{\lim_{a\to 0}} \frac{1}{\ln(P_1^z/P_2^z)} \ln \left[\frac{\int db^z e^{ib^z x P_1^z} P_1^z \sum_{\Gamma'} Z_{\Gamma\Gamma'}(\mu, a) \lim_{\ell\to\infty} W_{\mathcal{O}}^{\Gamma'}(b^z, b_\mathrm{T}, \ell, P_1^z, a)}{\int db^z e^{ib^z x P_2^z} P_2^z \sum_{\Gamma'} Z_{\Gamma\Gamma'}(\mu, a) \lim_{\ell\to\infty} W_{\mathcal{O}}^{\Gamma'}(b^z, b_\mathrm{T}, \ell, P_2^z, a)} \right]$$

$$+\delta\gamma_q(\mu, b_\mathrm{T}, P_1^z, P_2^z) + \mathcal{O}\left(\frac{1}{(xP^z b_\mathrm{T})^2}, \frac{M^2}{(xP^z)^2}, \frac{\Lambda_\mathrm{QCD}^2}{(xP^z)^2} \right)$$

EFT Matching Correction at NNLO, NLLL

Power corrections

(suppressed at lower mass)

X. Ji et. al, PRD91 (2015);
Ebert et. al, PRD99 (2019), JHEP09 (2019) 037;

Improved systematics in quasi-TMDs

TMD WFs in position space

$$\gamma_q(\mu, b_\mathrm{T}) = \boxed{\lim_{a\to 0}} \frac{1}{\ln(P_1^z/P_2^z)} \ln\left[\frac{\int db^z e^{ib^z x P_1^z} P_1^z \sum_{\Gamma'} Z_{\Gamma\Gamma'}(\mu, a) \lim_{\ell\to\infty} W_\mathcal{O}^{\Gamma'}(b^z, b_\mathrm{T}, \ell, P_1^z, a)}{\int db^z e^{ib^z x P_2^z} P_2^z \sum_{\Gamma'} Z_{\Gamma\Gamma'}(\mu, a) \lim_{\ell\to\infty} W_\mathcal{O}^{\Gamma'}(b^z, b_\mathrm{T}, \ell, P_2^z, a)}\right] + \delta\gamma_q(\mu, b_\mathrm{T}, P_1^z, P_2^z) + \boxed{\mathcal{O}\left(\frac{1}{(xP^z b_\mathrm{T})^2}, \frac{M^2}{(xP^z)^2}, \frac{\Lambda_\mathrm{QCD}^2}{(xP^z)^2}\right)}$$

- Defined via staple-shaped operators

$$\mathcal{O}^\Gamma(b_T, b^z, y, \ell) = \bar{d}\left(y + \frac{b}{2}\right)\frac{\Gamma}{2}\mathcal{W}_\sqsupset\left(y + \frac{b}{2}, y - \frac{b}{2}, \ell\right)u\left(y - \frac{b}{2}\right)$$

in hadron-to-vacuum matrix elements

$$\tilde{\phi}_\Gamma(b_T, b^z, P^z, \ell) \propto \langle 0|\mathcal{O}^\Gamma(b_T, b^z, y, \ell)\,|h(P^z)\rangle$$

extracted for each b_T, b^z, P^z, ℓ from two-point correlators — computationally intensive.

Potential improvements in Coulomb gauge? See Yong's talk from Monday

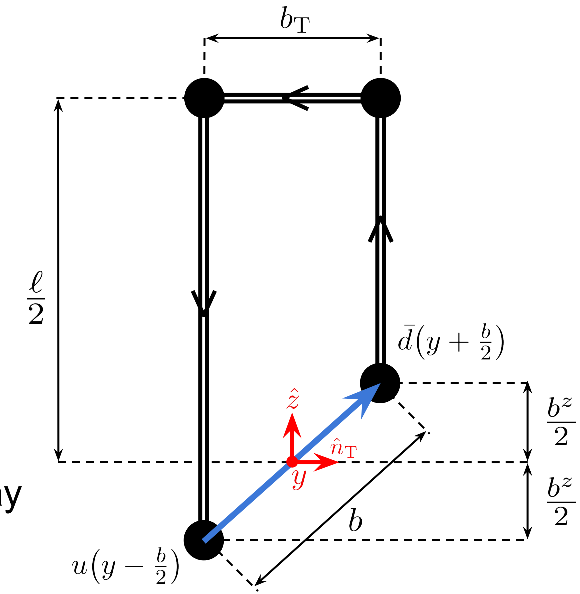

- Power divergences linear in the length of the Wilson line subtracted in WF ratios

$$W_\Gamma^{(0)}(b_T, b^z, P^z, \ell) = \frac{\tilde{\phi}_\Gamma(b_T, b^z, P^z, \ell)}{\tilde{\phi}_{\gamma^4\gamma^5}(b_T, 0, 0, \ell)}$$

Mixing effects quantified with RIxMOM

$$\gamma_q(\mu, b_\mathrm{T}) = \lim_{a\to 0} \frac{1}{\ln(P_1^z/P_2^z)} \ln \left[\frac{\int \mathrm{d}b^z e^{ib^z x P_1^z} P_1^z \sum_{\Gamma'} Z_{\Gamma\Gamma'}(\mu, a) \lim_{\ell\to\infty} W_{\mathcal{O}}^{\Gamma'}(b^z, b_\mathrm{T}, \ell, P_1^z, a)}{\int \mathrm{d}b^z e^{ib^z x P_2^z} P_2^z \sum_{\Gamma'} Z_{\Gamma\Gamma'}(\mu, a) \lim_{\ell\to\infty} W_{\mathcal{O}}^{\Gamma'}(b^z, b_\mathrm{T}, \ell, P_2^z, a)} \right] + \delta\gamma_q(\mu, b_\mathrm{T}, P_1^z, P_2^z) + \mathcal{O}\left(\frac{1}{(xP^z b_\mathrm{T})^2}, \frac{M^2}{(xP^z)^2}, \frac{\Lambda_\mathrm{QCD}^2}{(xP^z)^2} \right)$$

- Calculation of mixing effects in RIxMOM independent of staple geometry.

$$W_\Gamma^{\overline{\mathrm{MS}}}(b_T, \mu, b^z, P^z, \ell) = \sum_{\Gamma'} Z_{\Gamma\Gamma'}^{\overline{\mathrm{MS}}}(\mu)\, W_\Gamma^{(0)}(b_T, b^z, P^z, \ell)$$

- Full 16x16 mixing matrix computed

$$\mathcal{M}_{\Gamma\Gamma'}^{\mathrm{RI/xMOM}}(p_\mathrm{R},\ \xi_\mathrm{R}, a) \equiv \frac{\mathrm{Abs}[Z_{\Gamma\Gamma'}^{\mathrm{RI/xMOM}}(p_\mathrm{R}, \xi_\mathrm{R}, a)]}{\frac{1}{16}\sum_\Gamma \mathrm{Abs}[Z_{\Gamma\Gamma}^{\mathrm{RI/xMOM}}(p_\mathrm{R}, \xi_\mathrm{R}, a)]}$$

- Dominant mixings consistent with lattice perturbation theory at 1-loop.*

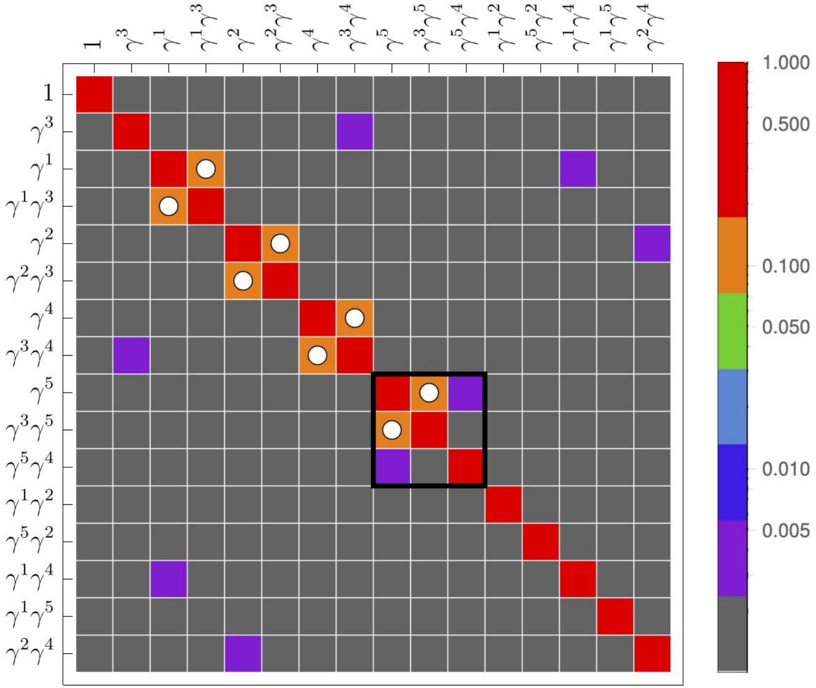

$$p_\mathrm{R}^\mu = \frac{2\pi}{L} \times (0, 0, 10, 0),\ \xi = 0.24\ \mathrm{fm}$$

X. Ji, et. al, PRL 120 (2018), [1706.08962]
J. Green et. al, PRL 121 (2018), [1707.07152]
J. Green et. al, PRD 101 (2020), [2002.09408]
*M. Constantinou et al., PRD 99 (2019), [1901.03862]
Y. Ji et. al., PRD 104 (2021), [2104.13345]
C. Alexandrou et al., [2305.11824]

See also talk by G. Spanoudes from Monday

TMD WFs in position space

$$\gamma_q(\mu, b_T) = \boxed{\lim_{a\to 0}} \frac{1}{\ln(P_1^z/P_2^z)} \ln\left[\frac{\int db^z e^{ib^z x P_1^z} P_1^z \sum_{\Gamma'} Z_{\Gamma\Gamma'}(\mu,a) \lim_{\ell\to\infty} W_{\mathcal{O}}^{\Gamma'}(b^z, b_T, \ell, P_1^z, a)}{\int db^z e^{ib^z x P_2^z} P_2^z \sum_{\Gamma'} Z_{\Gamma\Gamma'}(\mu,a) \lim_{\ell\to\infty} W_{\mathcal{O}}^{\Gamma'}(b^z, b_T, \ell, P_2^z, a)}\right] + \delta\gamma_q(\mu, b_T, P_1^z, P_2^z) + \boxed{\mathcal{O}\left(\frac{1}{(xP^z b_T)^2}, \frac{M^2}{(xP^z)^2}, \frac{\Lambda_{QCD}^2}{(xP^z)^2}\right)}$$

- Shown for bT = 0.48 fm, Pz = 1.29 GeV.
- Consistent between different staple lengths.
- Decay to zero within computed bz ranges

without mixing effects

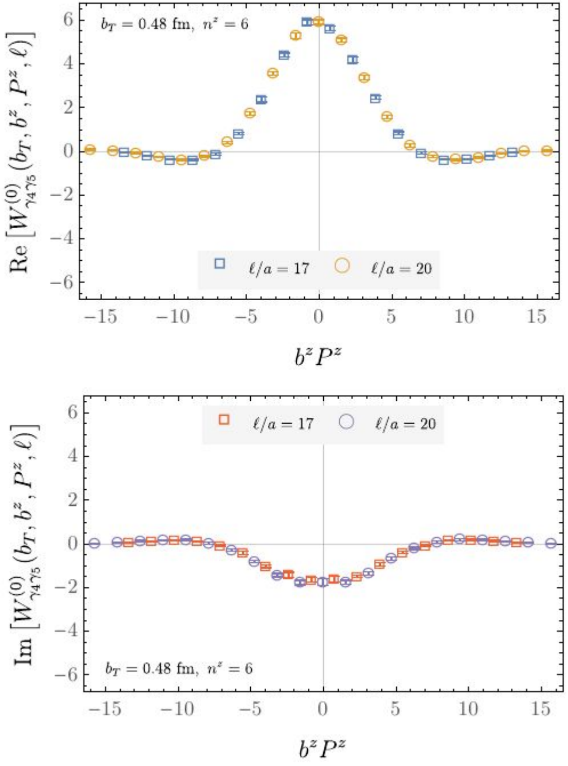

with mixing effects

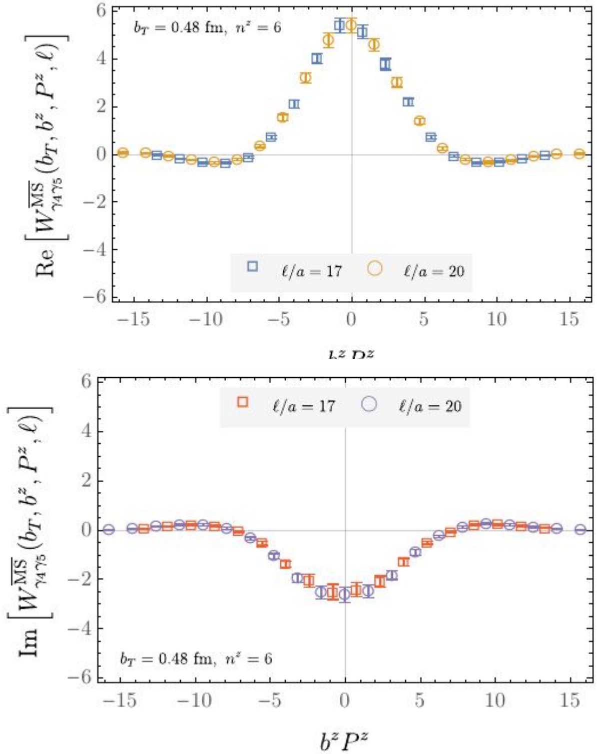

TMD WFs in momentum space

$$\gamma_q(\mu, b_T) = \boxed{\lim_{a\to 0}} \frac{1}{\ln(P_1^z/P_2^z)} \ln\left[\frac{\boxed{\int db^z e^{ib^z x P_1^z} P_1^z}\boxed{\sum_{\Gamma'} Z_{\Gamma\Gamma'}(\mu,a) \lim_{\ell\to\infty} W_{\mathcal{O}}^{\Gamma'}(b^z, b_T, \ell, P_1^z, a)}}{\boxed{\int db^z e^{ib^z x P_2^z} P_2^z}\boxed{\sum_{\Gamma'} Z_{\Gamma\Gamma'}(\mu,a) \lim_{\ell\to\infty} W_{\mathcal{O}}^{\Gamma'}(b^z, b_T, \ell, P_2^z, a)}}\right] \boxed{+\delta\gamma_q(\mu, b_T, P_1^z, P_2^z)} + \boxed{\mathcal{O}\left(\frac{1}{(xP^z b_T)^2}, \frac{M^2}{(xP^z)^2}, \frac{\Lambda_{QCD}^2}{(xP^z)^2}\right)}$$

bz range sufficient to use a Discrete Fourier Transform

$$\bar{W}_\Gamma^{\overline{\text{MS}}}(b_T, \mu, x, P^z) = \frac{P^z}{2\pi} N_\Gamma(P) \sum_{|b_z| \le b_z^{\max}} e^{i\left(x - \frac{1}{2}\right)P^z b^z} \bar{W}_\Gamma^{\overline{\text{MS}}}(b_T, \mu, b^z, P^z)$$

Normalization factor to compare between Dirac structures

The DFT is stable to decreasing the range in $b_T^{\max}$:

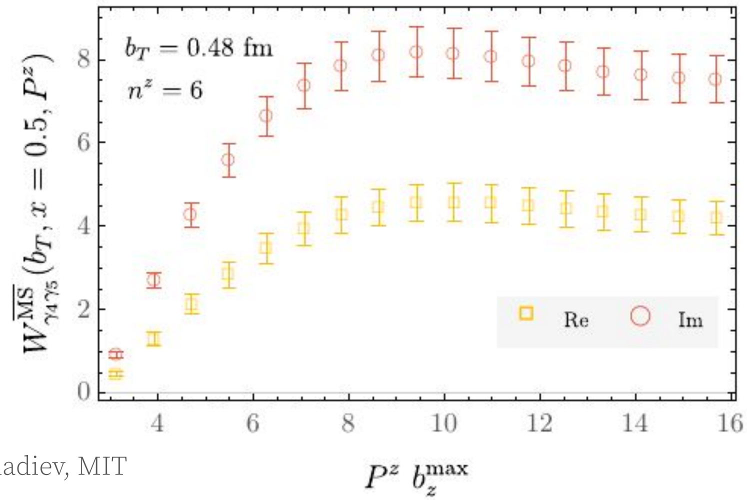

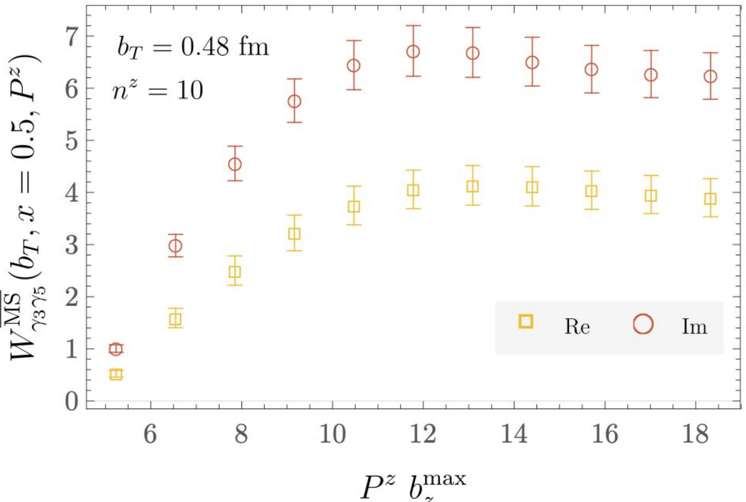

TMD WFs in momentum space

$$\gamma_q(\mu, b_{\mathrm{T}}) = \lim_{a\to 0}\frac{1}{\ln(P_1^z/P_2^z)}\ln\left[\frac{\int db^z e^{ib^z x P_1^z} P_1^z \sum_{\Gamma'} Z_{\Gamma\Gamma'}(\mu,a)\lim_{\ell\to\infty} W_{\mathcal{O}}^{\Gamma'}(b^z, b_{\mathrm{T}}, \ell, P_1^z, a)}{\int db^z e^{ib^z x P_2^z} P_2^z \sum_{\Gamma'} Z_{\Gamma\Gamma'}(\mu,a)\lim_{\ell\to\infty} W_{\mathcal{O}}^{\Gamma'}(b^z, b_{\mathrm{T}}, \ell, P_2^z, a)}\right] + \delta\gamma_q(\mu, b_{\mathrm{T}}, P_1^z, P_2^z) + \mathcal{O}\left(\frac{1}{(xP^z b_{\mathrm{T}})^2}, \frac{M^2}{(xP^z)^2}, \frac{\Lambda_{\mathrm{QCD}}^2}{(xP^z)^2}\right)$$

See convergence to the physical range $x \in [0,1]$ with increasing $P^z = \frac{2\pi}{L} n^z$

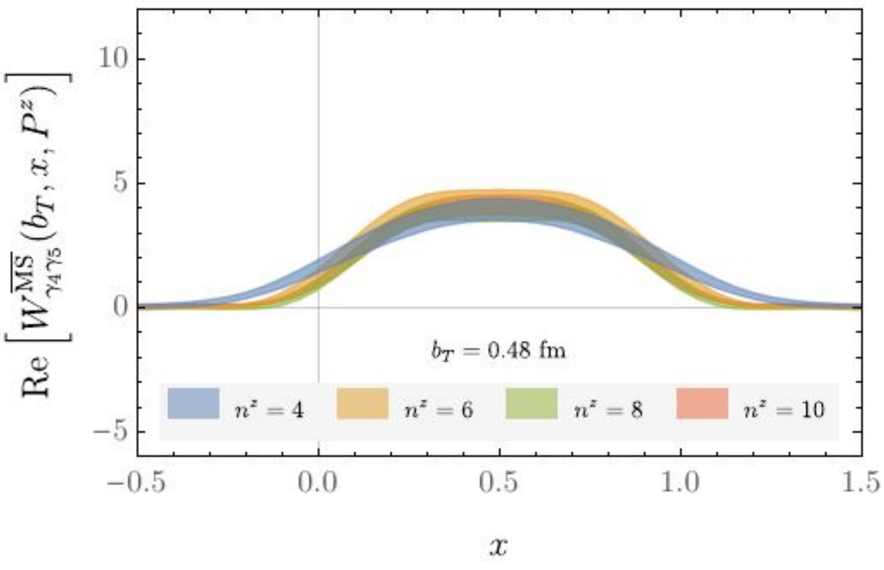

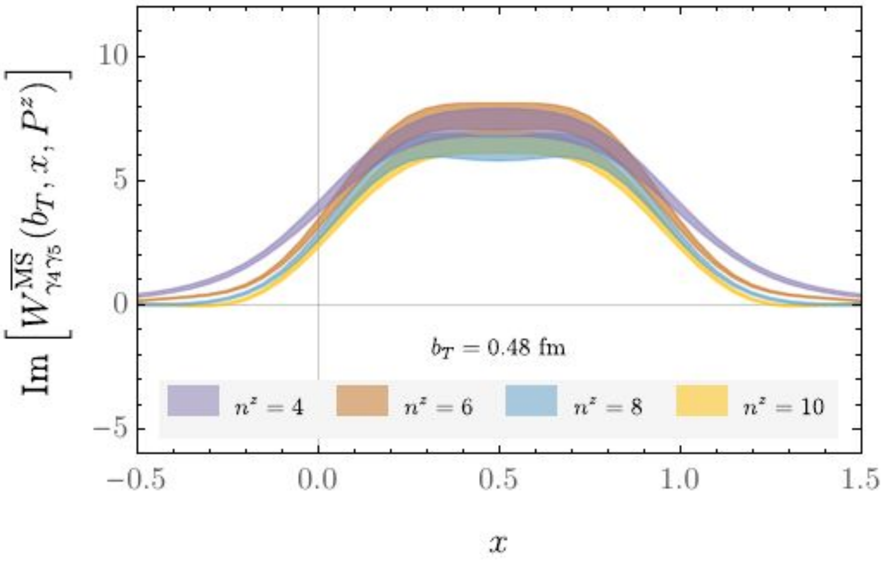

Non-zero imaginary part affects CS kernel estimates.

M.-H. Chu et al. (LPC), PRD 106, 034509, [2204.00200]
M.-H. Chu et al. (LPC), [2302.09961]
M.-H. Chu et al. (LPC), [2306.06488]

CS kernel estimates

$$\gamma_q(\mu, b_T) = \boxed{\lim_{a\to 0}} \frac{1}{\ln(P_1^z/P_2^z)} \ln \left[\frac{\boxed{\int db^z e^{ib^z x P_1^z} P_1^z} \boxed{\sum_{\Gamma'} Z_{\Gamma\Gamma'}(\mu, a) \lim_{\ell\to\infty} W_{\mathcal{O}}^{\Gamma'}(b^z, b_T, \ell, P_1^z, a)}}{\boxed{\int db^z e^{ib^z x P_2^z} P_2^z} \boxed{\sum_{\Gamma'} Z_{\Gamma\Gamma'}(\mu, a) \lim_{\ell\to\infty} W_{\mathcal{O}}^{\Gamma'}(b^z, b_T, \ell, P_2^z, a)}} \right] \boxed{+\delta\gamma_q(\mu, b_T, P_1^z, P_2^z)} + \boxed{\mathcal{O}\left(\frac{1}{(xP^z b_T)^2}, \frac{M^2}{(xP^z)^2}, \frac{\Lambda_{QCD}^2}{(xP^z)^2}\right)}$$

$$\hat{\gamma}_\Gamma^{\overline{\mathrm{MS}}}(b_T, x, P_1^z, P_2^z, \mu) = \frac{1}{\ln(P_1^z/P_2^z)} \ln \left[\frac{W_\Gamma^{\overline{\mathrm{MS}}}(b_T, x, P_1^z, \ell)}{W_\Gamma^{\overline{\mathrm{MS}}}(b_T, x, P_2^z, \ell)} \right] + \delta\gamma_q^{\overline{\mathrm{MS}}}(x, P_1^z, P_2^z, \mu)$$

X. Ji et. al., Phys. Lett. B 811 [1911.03840]
X. Ji and Y. Liu, PRD 105, [2106.05310]
Z.-F. Deng et. al, JHEP 09, [2207.07280]

- Cannot disentangle power corrections and O(a) effects at fixed lattice spacing.
- => average in $x \in [0.3, 0.7]$ separately for each momentum pair, bT, Dirac structure, and matching correction.
- Imaginary part explained by slower perturbative convergence and larger sensitivity to power corrections (next slides).

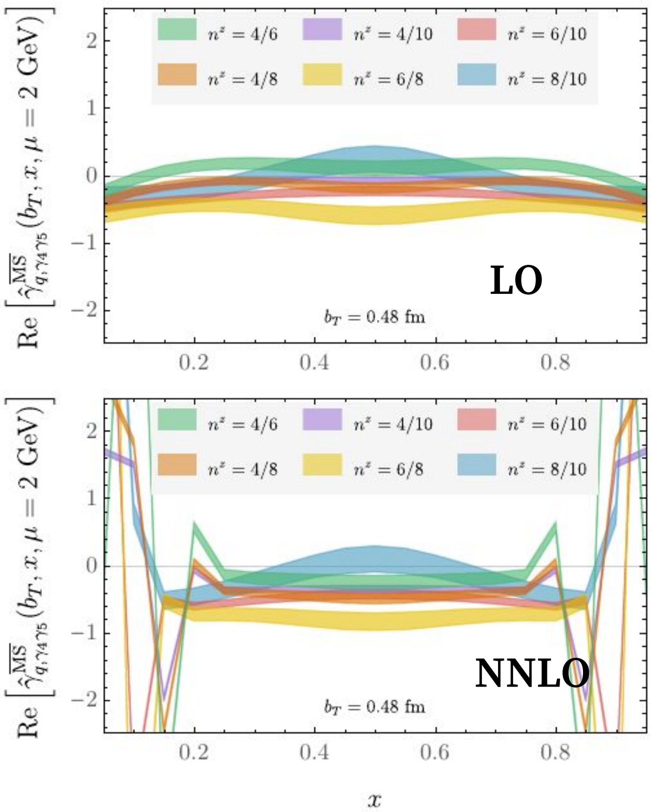

Better understanding of matching
and power corrections

Comparison of matching corrections

$$\gamma_q(\mu, b_\mathrm{T}) = \boxed{\lim_{a\to 0}} \frac{1}{\ln(P_1^z/P_2^z)} \ln \left[\frac{\int \mathrm{d}b^z e^{ib^z x P_1^z} P_1^z \sum_{\Gamma'} Z_{\Gamma\Gamma'}(\mu,a) \lim_{\ell\to\infty} W_{\mathcal{O}}^{\Gamma'}(b^z, b_\mathrm{T}, \ell, P_1^z, a)}{\int \mathrm{d}b^z e^{ib^z x P_2^z} P_2^z \sum_{\Gamma'} Z_{\Gamma\Gamma'}(\mu,a) \lim_{\ell\to\infty} W_{\mathcal{O}}^{\Gamma'}(b^z, b_\mathrm{T}, \ell, P_2^z, a)} \right] + \delta\gamma_q(\mu, b_\mathrm{T}, P_1^z, P_2^z) + \boxed{\mathcal{O}\left(\frac{1}{(xP^z b_\mathrm{T})^2}, \frac{M^2}{(xP^z)^2}, \frac{\Lambda_\mathrm{QCD}^2}{(xP^z)^2} \right)}$$

- New results at NNLO and NNLL.

O. del Río and A. Vladimirov, [2304.14440],

X. Ji et. al, [2305.04416].

Next talk after coffee break!

- $b_T \gtrsim 0.36\,\mathrm{fm}$: consistent between matching corrections
- $b_T \lesssim 0.36\,\mathrm{fm}$: deviations related to significant power corrections
- In the final **uNNLL** determination, combine matching corrections fron **NNLL** and **uNLO,**

  Where **uNLO** = fixed-order matching with bT-dependent terms vanishing $P^z b_T \gg 1$

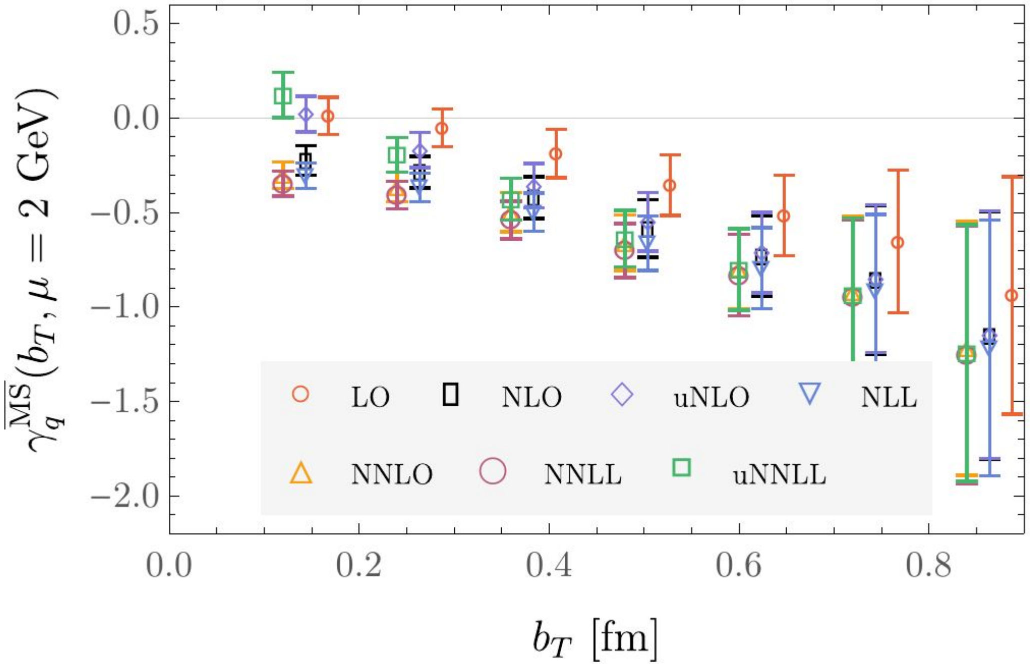

NLO, NNLO, and resummations

The correction is given by coefficients

$$\delta\gamma_q(x, P_1^z, P_2^z, \mu) \equiv \frac{1}{\ln(P_1^z/P_2^z)} \left(\ln \frac{C_\phi(xP_2^z, \mu)}{C_\phi(xP_1^z, \mu)} + (x \leftrightarrow \bar{x}) \right)$$

$C_\phi(p^z, \mu)$ appear in the TMD WF matching formula and are computed perturbatively as

$$C_\phi(p^z, \mu) = 1 + \sum_{n=1} \left(\frac{\alpha_s(\mu)}{4\pi} \right)^n C_\phi^{(n)}(p^z, \mu)$$

$$p^z \in xP^z, \bar{x}P^z$$

at LO, NLO and recently at NNLO, and resummed as

O. del Río and A. Vladimirov, [2304.14440]
X. Ji et. al, [2305.04416]

Resummation kernel

$$C_\phi(p^z, \mu) = C_\phi(p^z, 2p^z) \times \exp[K_\phi(p^z, 2p^z)]$$

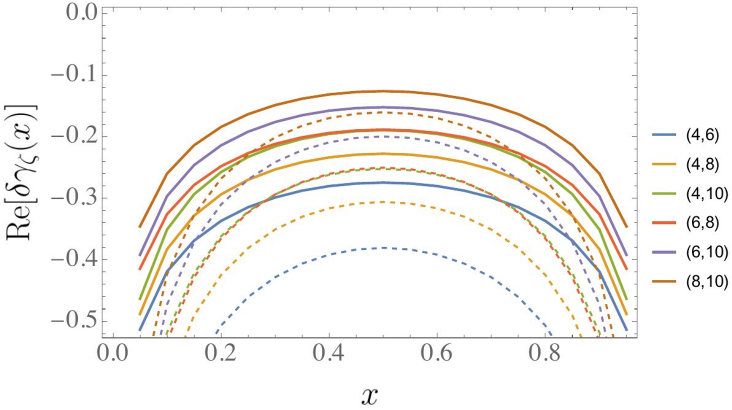

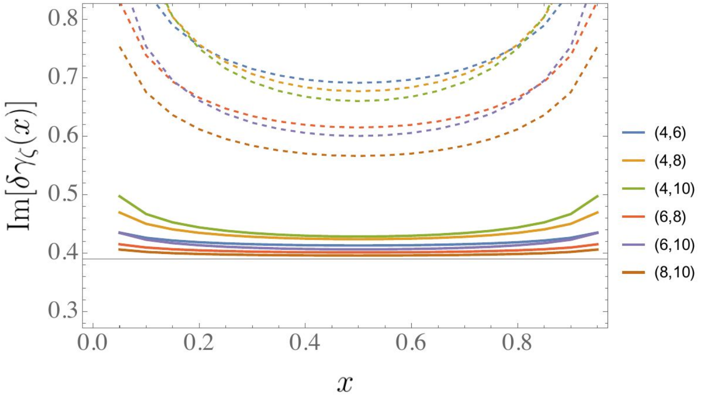

NLO (solid) and NNLO (dashed);
No convergence in the imaginary part

NLL and NNLL

X. Ji et. al., Phys. Lett. B 811 [1911.03840]
Ebert et. al, JHEP 04 (2022), [2201.08401]

Resummation kernel is $K_\phi(2p^z,\mu) = 2K_\Gamma(2p^z,\mu) - K_{\gamma_\mu}(2p^z,\mu) - i\pi\eta(2p^z,\mu)$

$$K_{\gamma_\mu}(\mu_0,\mu) = \int_{\alpha_s(\mu_0)}^{\alpha_s(\mu)} \frac{\mathrm{d}\alpha_s}{\beta(\alpha_s)}\gamma_\mu\,(\alpha_s),$$

$$K_\Gamma(\mu_0,\mu) = \int_{\alpha_s(\mu_0)}^{\alpha_s(\mu)} \frac{\mathrm{d}\alpha_s}{\beta(\alpha_s)}\Gamma_{\text{cusp}}(\alpha_s)\int_{\alpha_s(\mu_0)}^{\alpha_s} \frac{\mathrm{d}\alpha'_s}{\beta(\alpha'_s)},$$

$$\eta_\Gamma(\mu_0,\mu) = \int_{\alpha_s(\mu_0)}^{\alpha_s(\mu)} \frac{\mathrm{d}\alpha_s}{\beta(\alpha_s)}\Gamma_{\text{cusp}}(\alpha_s)$$

where $\Gamma_{\text{cusp}}(\alpha_s(\mu)) = \dfrac{\mathrm{d}\gamma_\mu\,(p^z,\mu)}{\mathrm{d}\ln p^z}$ and $\gamma_\mu(p^z,\mu) \equiv \dfrac{d\ln C_\phi(p^z,\mu)}{d\ln\mu}$

are computed perturbatively at following loop orders for each resummation accuracy:

	K_Γ	K_{γ_C}	K_{γ_μ}	η	C_ϕ
NLL	2	1	1	1	0
NNLL	3	2	2	2	1

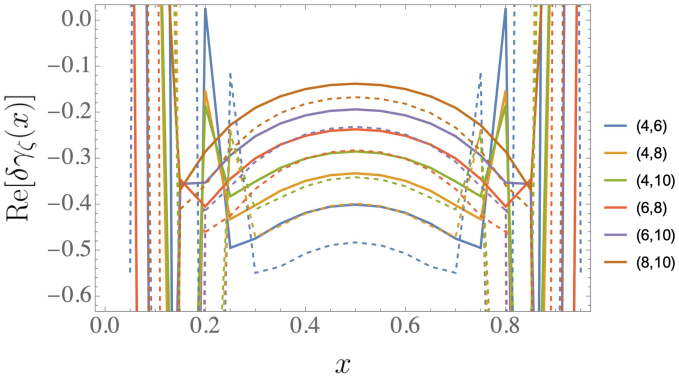

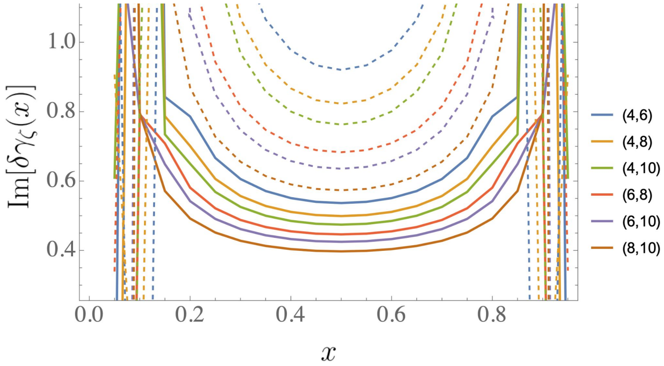

NLL (solid) and NNLL (dashed)
No convergence in the imaginary part

bT-dependent matching

Matching coefficients C included are a $P^z b_T \gg 1$ limit of

$$\boxed{\mathbf{C}_\phi(p^z, b_T, \mu) = C_\phi(p^z, \mu) + \delta C_\phi(p^z, b_T)}$$

uNLO

$$p^z \in xP^z, \bar{x}P^z$$

- $\delta C_\phi(p^z, b_T)$ contains bT-dependent terms on $x \in (-\infty, \infty)$ suppressed in $P^z b_T$
- Has been computed at NLO.

M. A. Ebert et. al,, JHEP 09, 037, [1901.03685]
Z.-F. Deng et. al, JHEP 09, [2207.07280]

- Corresponding unexpanded (in bT) matching correction reveals power corrections in 1/Pz bT.
- Imaginary part more sensitive to power corrections => <u>not taken as a systematic uncertainty directly.</u>

M.-H. Chu et al. (LPC), PRD 106, 034509, [2204.00200]
M.-H. Chu et al. (LPC), [2302.09961]
M.-H. Chu et al. (LPC), [2306.06488]

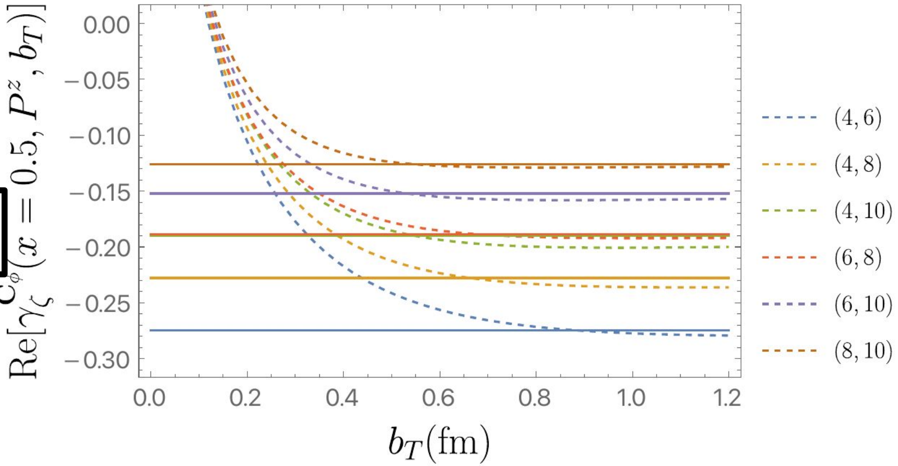

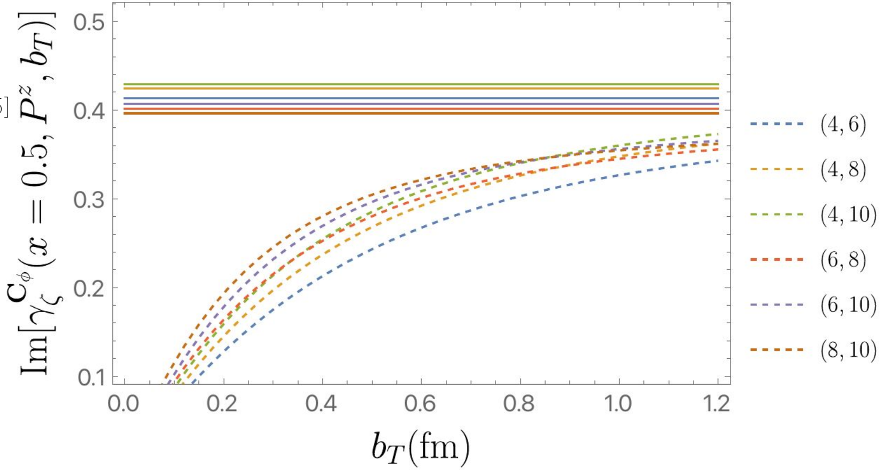

Dashed: **uNLO**, solid: NLO.

The imaginary part in the CS kernel estimate

- The CS kernel is real-valued.
- The CS kernel *estimate* has a non-zero imaginary part, primarily from matching.
- This is explained by poor perturbative convergence and power corrections in bT => not treated as a systematic directly

M.-H. Chu et al. (LPC), PRD 106, 034509, [2204.00200]
M.-H. Chu et al. (LPC), [2302.09961]
M.-H. Chu et al. (LPC), [2306.06488]

- Estimates of power corrections expected to improve with multiple lattice spacings, by disentangling O(a) effects
- For this calculation, uNNLL dominated by uNLO at small bT – unexpanded matching accounts for power corrections.

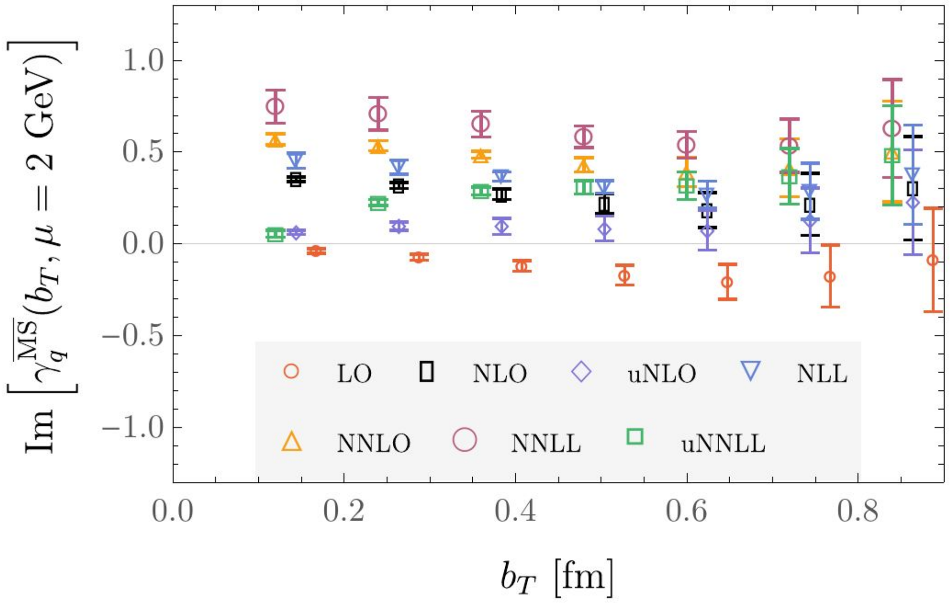

$$\boldsymbol{\delta\gamma_q}(x, b_T, P_1^z, P_2^z, \mu) = -\frac{1}{\ln(P_1^z/P_2^z)}\left(\ln\frac{C_\phi(xP_1^z, b_T, 2xP_1^z)}{C_\phi(xP_2^z, b_T, 2xP_2^z)} - (K_\phi(2xP_1^z, \mu) - K_\phi(2xP_2^z, \mu)) + (x \leftrightarrow \bar{x})\right)$$

Additional systematics from momenta and Dirac structures

- Momentum pairs combined in a weighted average

- Dirac structures differ by power corrections
- Averaged, difference added to systematics.

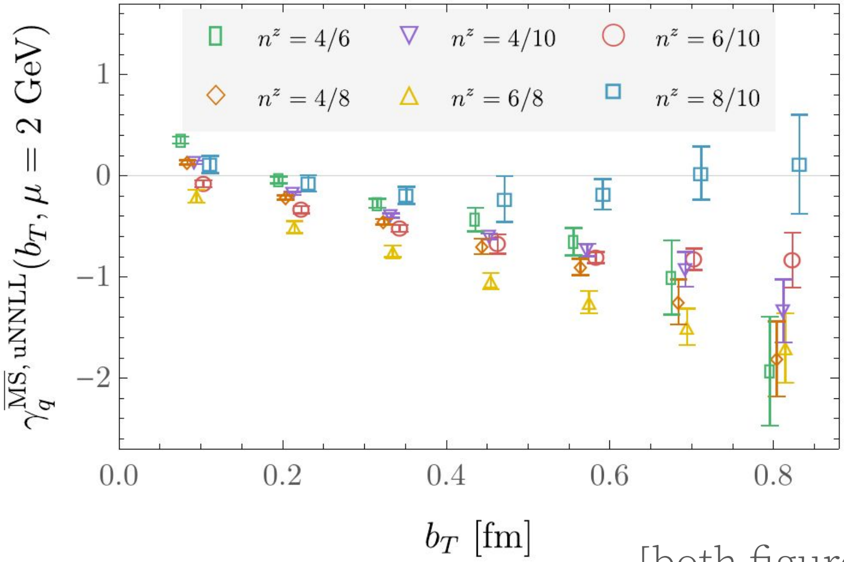

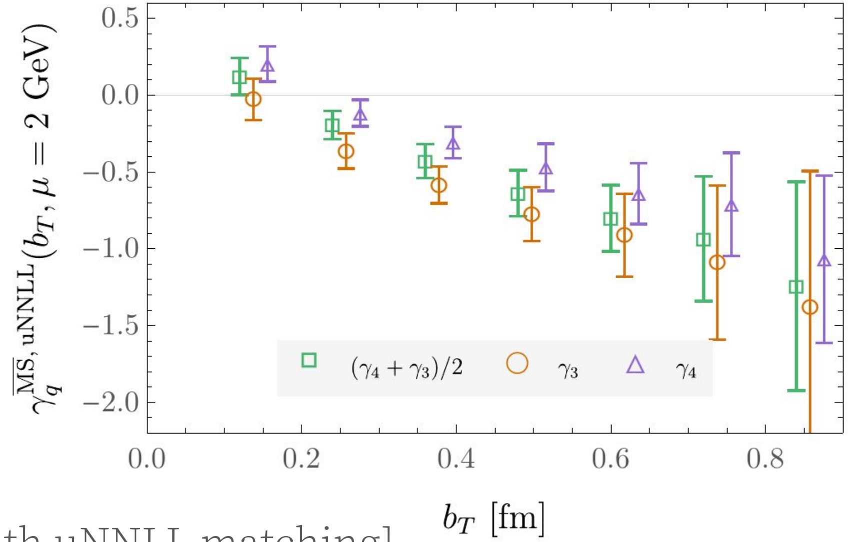

[both figures with uNNLL matching]

Conclusion and outlook

$$\gamma_q(\mu, b_\mathrm{T}) = \boxed{\lim_{a\to 0}} \frac{1}{\ln(P_1^z/P_2^z)} \ln\left[\frac{\boxed{\int db^z e^{ib^z x P_1^z} P_1^z} \boxed{\sum_{\Gamma'} Z_{\Gamma\Gamma'}(\mu,a) \lim_{\ell\to\infty} W_{\mathcal{O}}^{\Gamma'}(b^z, b_\mathrm{T}, \ell, P_1^z, a)}}{\boxed{\int db^z e^{ib^z x P_2^z} P_2^z} \boxed{\sum_{\Gamma'} Z_{\Gamma\Gamma'}(\mu,a) \lim_{\ell\to\infty} W_{\mathcal{O}}^{\Gamma'}(b^z, b_\mathrm{T}, \ell, P_2^z, a)}}\right]$$

$$\boxed{+\delta\gamma_q(\mu, b_\mathrm{T}, P_1^z, P_2^z)} + \boxed{\mathcal{O}\left(\frac{1}{(xP^z b_\mathrm{T})^2}, \frac{M^2}{(xP^z)^2}, \frac{\Lambda_{\mathrm{QCD}}^2}{(xP^z)^2}\right)}$$

- First calculation at ~physical pion mass $M_\pi \approx 150\,\mathrm{MeV}$ and NNLO+NNLL matching, improved systematics.
- Precision sufficient to begin to discriminate between global analyses
- Perturbative convergence for bT > .36 fm
- Power corrections for bT < .36 fm accounted by unexpanded matching.
- **Significant progress from the 2021 calculation.**
- Next steps: better quantify power corrections by disentangling O(a) effects at multiple lattice spacings.

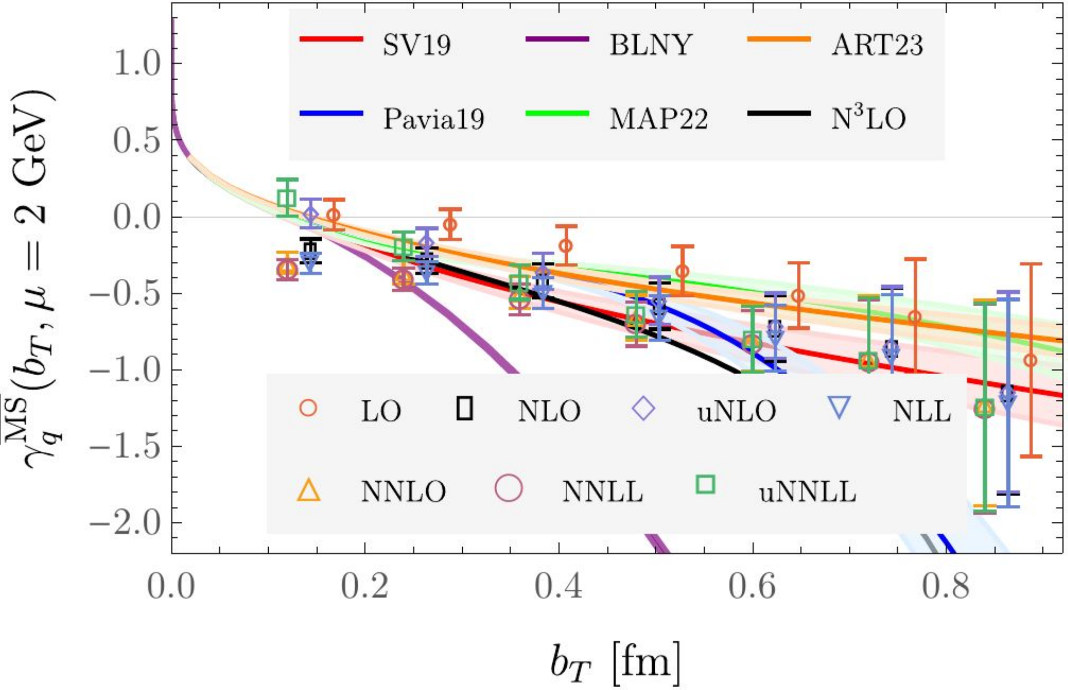

Backup slides

TMD WFs in position space

$$\gamma_q(\mu, b_T) = \boxed{\lim_{a\to 0}} \frac{1}{\ln(P_1^z/P_2^z)} \ln \left[\frac{\boxed{\int db^z e^{ib^z x P_1^z} P_1^z} \boxed{\sum_{\Gamma'} Z_{\Gamma\Gamma'}(\mu, a) \lim_{\ell\to\infty} W_{\mathcal{O}}^{\Gamma'}(b^z, b_T, \ell, P_1^z, a)}}{\boxed{\int db^z e^{ib^z x P_2^z} P_2^z} \boxed{\sum_{\Gamma'} Z_{\Gamma\Gamma'}(\mu, a) \lim_{\ell\to\infty} W_{\mathcal{O}}^{\Gamma'}(b^z, b_T, \ell, P_2^z, a)}} \right] \boxed{+\delta\gamma_q(\mu, b_T, P_1^z, P_2^z)} \boxed{+ \mathcal{O}\left(\frac{1}{(xP^z b_T)^2}, \frac{M^2}{(xP^z)^2}, \frac{\Lambda_{QCD}^2}{(xP^z)^2} \right)}$$

Statistical noise makes computation challenging for large $P^z, \ell,$ and b_T

- $b_T = 0.48\,\text{fm},\ 0.84\,\text{fm}$ left to right
- $P^z = 2.15\,\text{GeV},\ 1.72\,\text{GeV}$ top to bottom
- Our group's previous calculation had $b_T^{\max} = 0.48\,\text{fm}$, $P^z_{\max} = 1.51\,\text{GeV}$

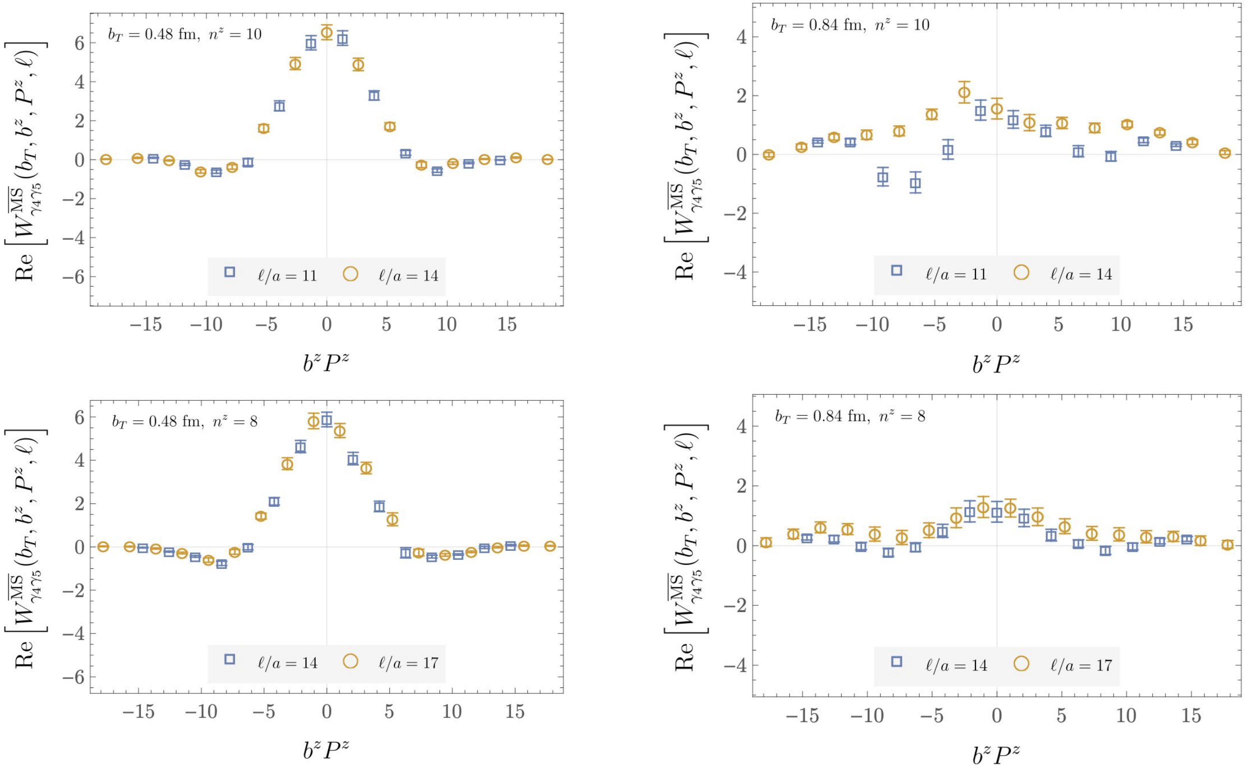

TMD WFs in momentum space

$$\gamma_q(\mu, b_T) = \boxed{\lim_{a\to 0}} \frac{1}{\ln(P_1^z/P_2^z)} \ln \left[\frac{\boxed{\int db^z e^{ib^z x P_1^z} P_1^z} \boxed{\sum_{\Gamma'} Z_{\Gamma\Gamma'}(\mu, a) \lim_{\ell\to\infty} W_{\mathcal{O}}^{\Gamma'}(b^z, b_T, \ell, P_1^z, a)}}{\boxed{\int db^z e^{ib^z x P_2^z} P_2^z} \boxed{\sum_{\Gamma'} Z_{\Gamma\Gamma'}(\mu, a) \lim_{\ell\to\infty} W_{\mathcal{O}}^{\Gamma'}(b^z, b_T, \ell, P_2^z, a)}} \right]$$
$$\boxed{+\delta\gamma_q(\mu, b_T, P_1^z, P_2^z)} + \boxed{\mathcal{O}\left(\frac{1}{(xP^z b_T)^2}, \frac{M^2}{(xP^z)^2}, \frac{\Lambda_{\mathrm{QCD}}^2}{(xP^z)^2} \right)}$$

See convergence to the physical range $x \in [0, 1]$ with increasing $P^z = \frac{2\pi}{L} n^z$

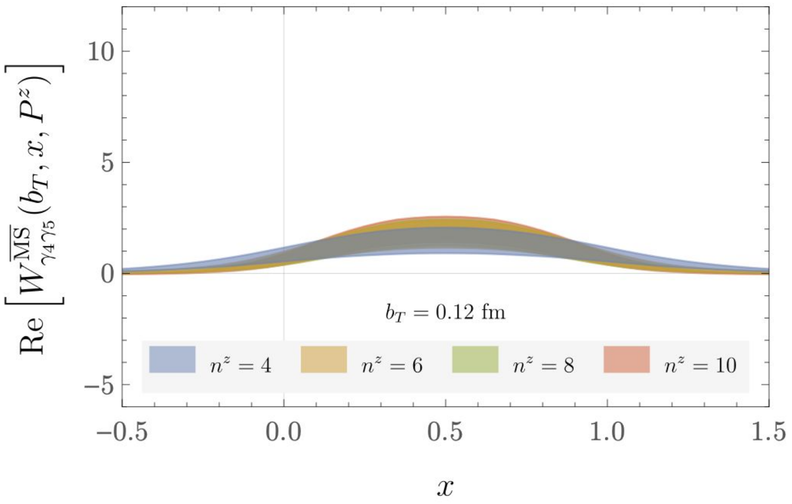

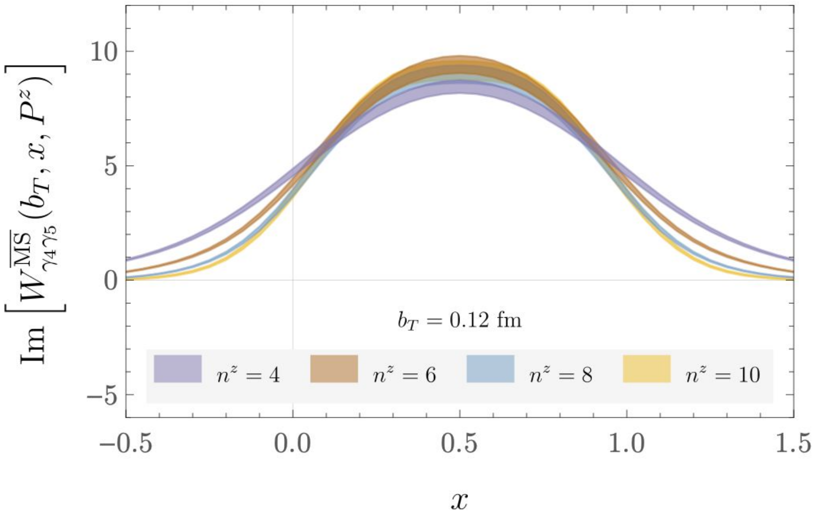

Non-zero imaginary part affects CS kernel estimates.

M.-H. Chu et al. (LPC), PRD 106, 034509, [2204.00200]
M.-H. Chu et al. (LPC), [2302.09961]
M.-H. Chu et al. (LPC), [2306.06488]

TMD WFs in momentum space

$$\gamma_q(\mu, b_T) = \boxed{\lim_{a\to 0}} \frac{1}{\ln(P_1^z/P_2^z)} \ln \left[\frac{\boxed{\int db^z e^{ib^z x P_1^z} P_1^z} \boxed{\sum_{\Gamma'} Z_{\Gamma\Gamma'}(\mu, a) \lim_{\ell\to\infty} W_{\mathcal{O}}^{\Gamma'}(b^z, b_T, \ell, P_1^z, a)}}{\boxed{\int db^z e^{ib^z x P_2^z} P_2^z} \boxed{\sum_{\Gamma'} Z_{\Gamma\Gamma'}(\mu, a) \lim_{\ell\to\infty} W_{\mathcal{O}}^{\Gamma'}(b^z, b_T, \ell, P_2^z, a)}} \right] \boxed{+\delta\gamma_q(\mu, b_T, P_1^z, P_2^z)} \boxed{+ \mathcal{O}\left(\frac{1}{(xP^z b_T)^2}, \frac{M^2}{(xP^z)^2}, \frac{\Lambda_{QCD}^2}{(xP^z)^2} \right)}$$

See convergence to the physical range $x \in [0, 1]$ with increasing $P^z = \frac{2\pi}{L} n^z$

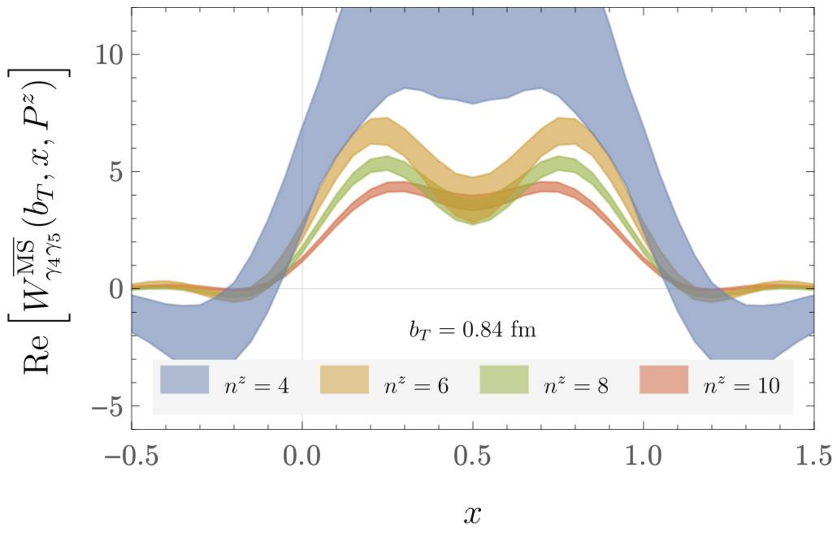

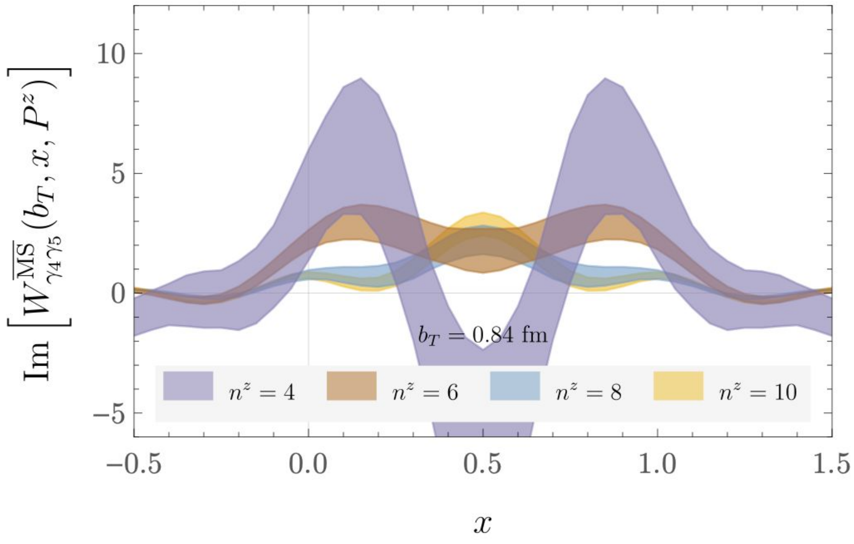

Non-zero imaginary part affects CS kernel estimates.

M.-H. Chu et al. (LPC), PRD 106, 034509, [2204.00200]
M.-H. Chu et al. (LPC), [2302.09961]
M.-H. Chu et al. (LPC), [2306.06488]

Using auxiliary fields for non-perturbative renormalization

Get a renormalized staple-shaped operator

$$\mathcal{O}^{\text{ren.}}_{\ell,\Gamma} = Z^{\text{ren.}}_{\mathcal{O}_\ell \Gamma\Gamma'} \mathcal{O}^{\text{bare}}_{\ell,\Gamma}$$

By solving for Z_O in a renormalization scheme where it is given by matrix elements computed non-perturbatively, such as

$$\Lambda^{\text{bare}}_{\ell,\Gamma}(p,b) = \langle q(p)|\mathcal{O}^{\text{bare}}_{\ell,\Gamma}(b)|q(p)\rangle_{\text{gf,amp.}}$$

renormalized as

$$\Lambda^{\text{RI}'-\text{MOM}}_{\ell,\Gamma}(p,b) = [Z_q'(p)]^{-1} Z^{\text{RI}'-\text{MOM}}_{\mathcal{O}_\ell(b),\Gamma\Gamma'}(p)\Lambda^{\text{bare}}_{\ell,\Gamma}(p,b)$$

Set to its tree-level value at p = p_R, together with some renormalization condition for Z_q. This is RI'-MOM, *with a different Z_O for each staple configuration.*

[1]Green, Jansen, and Steffens, PRL 121 (2018) and PRD 101(2020).

With the auxiliary-field approach, renormalization of extended staples is simplified to that of point-like objects:

$$\begin{aligned}
&\bar{q}(b)\,\Gamma W_{-z} W_{\mathrm{T}} W_{+z}\, q(0) \\
&\quad = \langle \bar{q}(b)\ \underbrace{\Gamma\zeta_{-z}(b)\bar{\zeta}_{-z}(\eta+b_{\mathrm{T}})}_{W_{-z}}\,\underbrace{\zeta_{\mathrm{T}}(\eta+b_{\mathrm{T}})\bar{\zeta}_{\mathrm{T}}(\eta)}_{W_{\mathrm{T}}}\,\underbrace{\zeta_{+z}(\eta)\bar{\zeta}_{+z}(0)}_{W_{+z}}\ q(0)\rangle_\zeta \\
&\quad = \langle \underbrace{\bar{q}(b)\zeta_{-z}(b)}_{\phi_{-z}(b)}\,\Gamma\,\underbrace{\bar{\zeta}_{-z}(\eta+b_{\mathrm{T}})\zeta_{\mathrm{T}}(\eta+b_{\mathrm{T}})}_{C_{-z,\mathrm{T}}(\eta+b_{\mathrm{T}})}\,\underbrace{\bar{\zeta}_{\mathrm{T}}(\eta)\zeta_{+z}(\eta)}_{C_{\mathrm{T},+z}(\eta)}\,\underbrace{\bar{\zeta}_{+z}(0)q(0)}_{\phi_{+z}(0)}\rangle_\zeta
\end{aligned}$$

where Wilson lines are given by zeta propagators in the extended theory, and Z_0 is broken down as

$$\begin{aligned}
\mathcal{O}^{\text{ren.}}_{\ell,\Gamma} &= e^{-\delta m(l+b_{\mathrm{T}})}(Z^\dagger_{\phi_{-z}}\Gamma Z_{\phi_{+z}}) \\
&\quad\times \langle \phi_{-z}(Z_{C_{-z,\mathrm{T}}}C_{-z,\mathrm{T}})(Z_{C_{\mathrm{T},+z}}C_{\mathrm{T},+z})\phi_{+z}\rangle_\zeta
\end{aligned}$$

with one renormalization condition for each Z, independent of staple configurations. This is RI-xMOM[1].

New renormalization scheme leads to reduced mixing

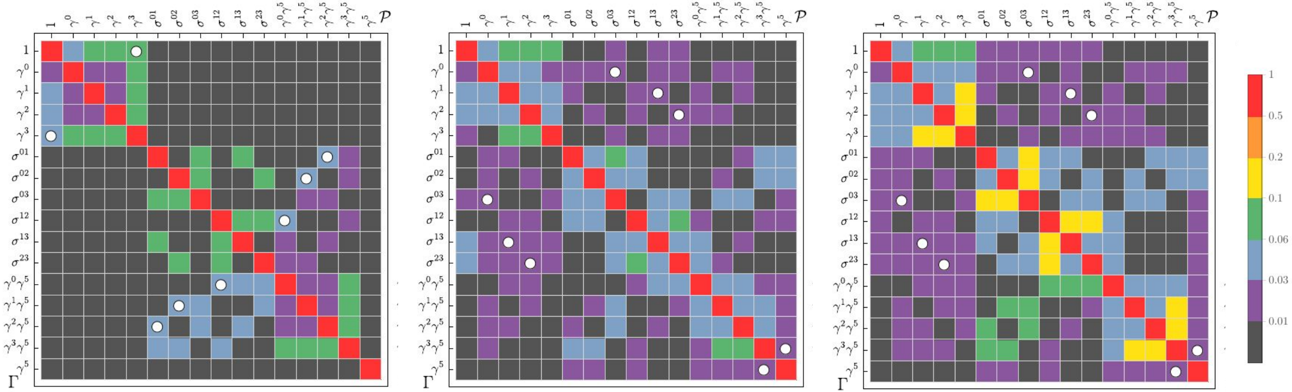

Figures from Shanahan, Wagman, and Zhao, PRD 101 (2020)

Showing mixing patterns for RI'-MOM from left to right for: straight-line, symmetric, and asymmetric staples.

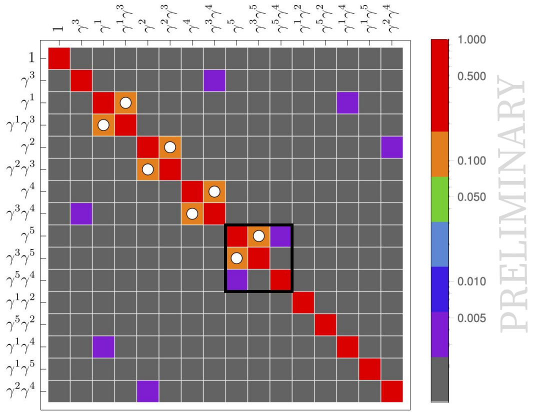

$p_R^\mu = \frac{2\pi}{L} \times (0, 0, 10, 0)$, $\xi = 0.24$ fm

For short, straight-line configurations, mixing patterns in RI'-MOM agree with lattice perturbation theory at one-loop[1] (white circles), but deviations become large for staple-shaped Wilson lines; in comparison, mixing effects in RI-xMOM are well-controlled (for collinear momenta and Wilson lines)

[1] Constantinou, Panagopoulos, and Spanoudes, PRD 99 (2019) and PRD 96 (2017).

Preliminary figure from this work (different ensemble and renormalization scale)

Scheme dependence of mixing patterns

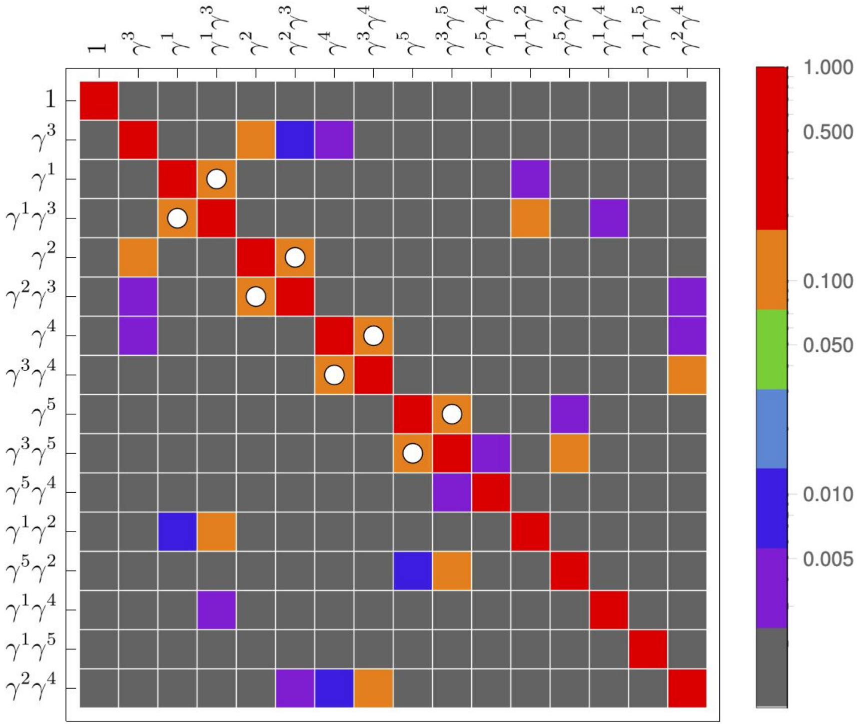

$$p_{\mathrm{R}}^{\mu} = \frac{2\pi}{L} \times (0, 10, 0, 0),\ \xi = 0.24\ \mathrm{fm}$$

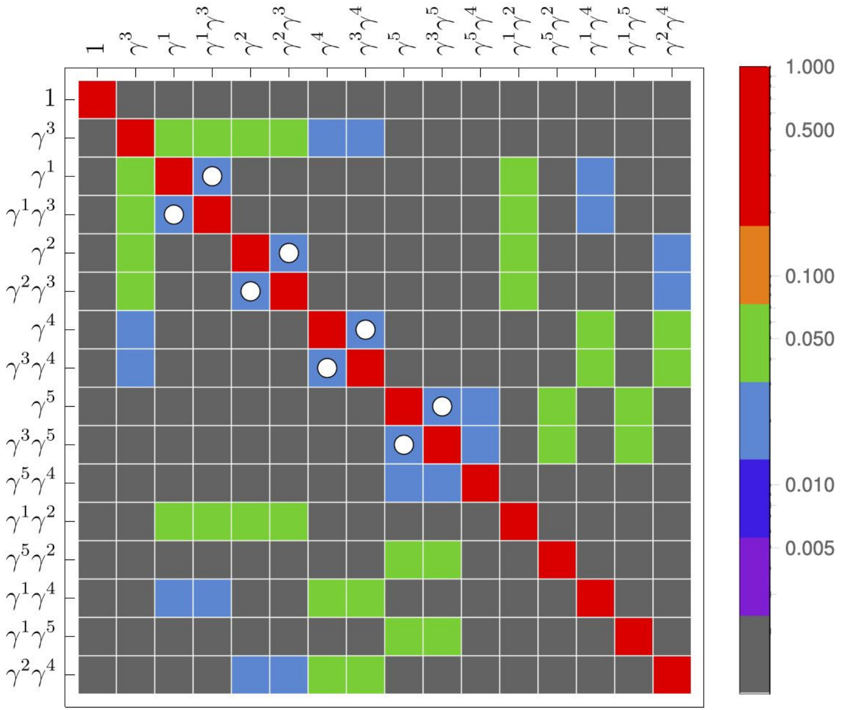

$$p_{\mathrm{R}}^{\mu} = \frac{2\pi}{L} \times (6, 6, 6, 6),\ \xi = 0.24\ \mathrm{fm}$$

Code improvements